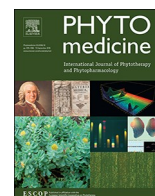




Since January 2020 Elsevier has created a COVID-19 resource centre with free information in English and Mandarin on the novel coronavirus COVID-19. The COVID-19 resource centre is hosted on Elsevier Connect, the company's public news and information website.

Elsevier hereby grants permission to make all its COVID-19-related research that is available on the COVID-19 resource centre - including this research content - immediately available in PubMed Central and other publicly funded repositories, such as the WHO COVID database with rights for unrestricted research re-use and analyses in any form or by any means with acknowledgement of the original source. These permissions are granted for free by Elsevier for as long as the COVID-19 resource centre remains active.



## Original Article

# Phillyrin (KD-1) exerts anti-viral and anti-inflammatory activities against novel coronavirus (SARS-CoV-2) and human coronavirus 229E (HCoV-229E) by suppressing the nuclear factor kappa B (NF- $\kappa$ B) signaling pathway



Qinhai Ma<sup>a,1</sup>, Runfeng Li<sup>a</sup>, Weiqi Pan<sup>a</sup>, Wenbo Huang<sup>a</sup>, Bin Liu<sup>e</sup>, Yuqi Xie<sup>a</sup>, Zhoulang Wang<sup>a</sup>, Chufang Li<sup>a</sup>, Haiming Jiang<sup>a</sup>, Jicheng Huang<sup>d</sup>, Yongxia Shi<sup>d</sup>, Jun Dai<sup>d</sup>, Kui Zheng<sup>d</sup>, Xiaobo Li<sup>d</sup>, Min Hui<sup>f</sup>, Li Fu<sup>f</sup>, Zifeng Yang<sup>a,b,c,\*</sup>

<sup>a</sup> State Key Laboratory of Respiratory Disease, National Clinical Research Center for Respiratory Disease, Guangzhou Institute of Respiratory Health, the First Affiliated Hospital of Guangzhou Medical University, Guangzhou, Guangdong, China

<sup>b</sup> State Key Laboratory of Quality Research in Chinese Medicine, Macau Institute for Applied Research in Medicine and Health, Macau University of Science and Technology, Taipa, Macau SAR, China

<sup>c</sup> KingMed Virology Diagnostic & Translational Center, Guangzhou, China

<sup>d</sup> Technology Centre, Guangzhou Customs, Guangzhou, China

<sup>e</sup> Kunming University of Science and Technology Library, Kunming, China

<sup>f</sup> Jilin Yatai Chinese Medicine Development Institute, Changchun, Jilin, China

## ARTICLE INFO

## Keywords:

Phillyrin (KD-1)

SARS-CoV-2

Antiviral

Anti-inflammatory

NF- $\kappa$ B

## ABSTRACT

**Background:** Severe acute respiratory syndrome coronavirus 2 (SARS-CoV-2) has extensively and rapidly spread in the world, causing an outbreak of acute infectious pneumonia. However, no specific antiviral drugs or vaccines can be used. Phillyrin (KD-1), a representative ingredient of *Forsythia suspensa*, possesses anti-inflammatory, anti-oxidant, and antiviral activities. However, little is known about the antiviral abilities and mechanism of KD-1 against SARS-CoV-2 and human coronavirus 229E (HCoV-229E).

**Purpose:** The study was designed to investigate the antiviral and anti-inflammatory activities of KD-1 against the novel SARS-CoV-2 and HCoV-229E and its potential effect in regulating host immune response *in vitro*.

**Methods:** The antiviral activities of KD-1 against SARS-CoV-2 and HCoV-229E were assessed in Vero E6 cells using cytopathic effect and plaque-reduction assay. Proinflammatory cytokine expression levels upon infection with SARS-CoV-2 and HCoV-229E infection in Huh-7 cells were measured by real-time quantitative PCR assays. Western blot assay was used to determine the protein expression of nuclear factor kappa B (NF- $\kappa$ B) p65, p-NF- $\kappa$ B p65, I $\kappa$ B $\alpha$ , and p-I $\kappa$ B $\alpha$  in Huh-7 cells, which are the key targets of the NF- $\kappa$ B pathway.

**Results:** KD-1 could significantly inhibit SARS-CoV-2 and HCoV-229E replication *in vitro*. KD-1 could also markedly reduce the production of proinflammatory cytokines (TNF- $\alpha$ , IL-6, IL-1 $\beta$ , MCP-1, and IP-10) at the mRNA levels. Moreover, KD-1 could significantly reduce the protein expression of p-NF- $\kappa$ B p65, NF- $\kappa$ B p65, and p-I $\kappa$ B $\alpha$ , while increasing the expression of I $\kappa$ B $\alpha$  in Huh-7 cells.

**Conclusions:** KD-1 could significantly inhibit virus proliferation *in vitro*, the up-regulated expression of proin-

**Abbreviations:** COVID-19, new coronavirus disease; CPE, Cytopathic effect; EC50, 50 % effective concentration; FBS, Foetal bovine serum; G-CSF, Granulocyte colony-stimulating factor; GAPDH, Glyceraldehyde 3-phosphate dehydrogenase; HPLC, High-performance liquid chromatography; HCoV-229E, Human coronavirus 229E; IL-1 $\beta$ , Interleukin-1beta; IL-6, Interleukin-6; IP-10, Interferon-inducible protein-10; VERO E6 cells, Monkey kidney cell line; KD-1, Phillyrin; MERS-CoV, Middle East respiratory syndrome coronavirus; MIP-1 $\alpha$ , Recombinant Macrophage Inflammatory Protein 1 Alpha; MTT, Methyl thiazolyl tetrazolium; MCP-1, Monocyte chemoattractant protein-1; PBS, Phosphate-buffered saline; RT-PCR, Real-time polymerase chain reaction; SARS-CoV, Severe acute respiratory syndrome coronavirus; SARS-CoV-2, Severe Acute Respiratory Syndrome Coronavirus 2; TNF- $\alpha$ , Tumor necrosis factor- $\alpha$ ; TCM, Traditional Chinese medicine; TC50, 50 % toxicity concentration; TCID50, 100  $\times$  50% tissue culture infective dose

\* Corresponding author.

E-mail address: [jeffyah@163.com](mailto:jeffyah@163.com) (Z. Yang).

<sup>1</sup> Qinhai Ma, Runfeng Li have equal contributions to this study.

<https://doi.org/10.1016/j.phymed.2020.153296>

Received 13 March 2020; Received in revised form 21 July 2020; Accepted 31 July 2020

0944-7113/ © 2020 Elsevier GmbH. All rights reserved.

flammatory cytokines induced by SARS-CoV-2 and HCoV-229E by regulating the activity of the NF- $\kappa$ B signaling pathway. Our findings indicated that KD-1 protected against virus attack and can thus be used as a novel strategy for controlling the coronavirus disease 2019.

## Introduction

Coronaviruses (CoVs), which belong to the family Coronaviridae, are positive-sense single-stranded RNA viruses, that infect numerous animals, including birds and mammals (Ksiazek et al., 2003). CoVs are common pathogens that easily cause respiratory tract infection and induce different degrees of diseases. These diseases range from upper respiratory tract infections with mild symptoms to lower respiratory tract infections with severe symptoms, including acute tracheitis, pneumonia, bronchitis, and even severe acute respiratory syndrome (SARS) (Heimdal et al., 2019; Owusu et al., 2014; Xu et al., 2020). SARS-CoV-2 (formerly known as 2019-nCoV, the causative pathogen of coronavirus disease 2019 (COVID-19), has widely and rapidly spread in the world, causing an outbreak of acute infectious pneumonia (Du, 2020; Carlos et al., 2020). COVID-19 is a major CoV infection that has threatened human life after SARS and Middle East respiratory syndrome (MERS), causing severe respiratory illness and even death (Zaki et al., 2012). Despite a series of extraordinary social-alienation measures in various countries, the number of people infected continues to rise. Moreover, the population's susceptibility to these highly pathogenic CoVs has contributed to large outbreaks and evolved into public health events: thereby highlighting the necessity to prepare for future re-emergence or novel emerging viruses (Nkengasong, 2020). For this sudden and lethal disease, no specific antiviral drugs or vaccines can be used. Therefore, identifying effective antiviral agents to combat the disease is urgently needed.

At present, some drugs can effectively eliminate SARS-CoV-2 and improve symptoms. These drugs are reportedly effective *in vitro*, such as fusion peptide (EK1) (Xia et al., 2019), abidol (Coleman et al., 2016), RNA-synthesis inhibitors (eg., TDF and 3TC), and anti-inflammatory drugs (eg., hormones and other molecules). However, the efficacy and safety of drugs for SARS-CoV-2 pneumonia patients require further assessment through clinical trials.

A novel CoV pneumonia diagnosis and treatment plan jointly issued by the National Health Committee of the People's Republic of China and the National Administration of traditional Chinese medicine has classified COVID-19 into the category of "pestilence" in Traditional Chinese Medicine (TCM). In the third edition, part of "TCM treatment" for COVID-19 has been added, whereas the sixth edition describes the syndromes, tongue picture, and pulse throughout different periods of the disease, as well as recommends the relevant prescriptions and proprietary Chinese medicine. A previous report has indicated that the respiratory symptoms of four patients with mild or severe COVID-19 were cured or significantly improved after treatment with lopinavir/ritonavir, abidol, and Shufeng Jiedu Capsule on the basis of supportive nursing. Another retrospective analysis of clinical records conducted in SARS-CoV-2 infected patients at Wuhan Ninth Hospital and CR & WISCO General Hospital has shown that Lianhuaqingwen combination could significantly relieve cardinal symptoms and reduce the course of COVID-19 (Yao et al., 2020). Accordingly, studying the TCMs that have obvious advantages in the treating the new virus is important.

*Forsythia suspensa* (Thunb.) is a popular traditional Chinese medicine used to treat pyrexia and infections (Guo et al., 2007; Lua et al., 2010). Phillyrin (KD-1), a representative ingredient of *F. suspensa*, has anti-inflammatory (Diaz et al., 2001), anti-oxidant (Lee et al., 2011; Gulcin et al., 2006), and antiviral activities (Chen et al., 2004). A previous report has showed that KD-1 could inhibit inflammation in LPS-stimulated RAW264.7 macrophages *in vitro*, which is supposed to be linked with the restrained JAK-STAT and p38 MAPK signal pathways and decreased expression of ROS (Pan et al., 2014). KD-1 shows

phosphodiesterase-4 inhibitory activities in phosphodiesterase assay and reduces LPS-mediated TNF release in RAW264.7 and PBMC cells *in vitro* (Coon et al., 2014). Moreover, KD-1 (10, 20 mg/kg) suppresses the pulmonary histopathologic changes, alveolar hemorrhage, and neutrophil infiltration in an acute lung-injury mice model *in vivo*. It exerts protective effects against lung inflammation by down-regulating the contents of TNF- $\alpha$ , IL-1 $\beta$ , IL-6, and myeloperoxidase (Zhong et al., 2013). We have also found that KD-1 exerts antiviral effects in different respiratory tract viruses, including influenza virus, parainfluenza virus, and respiratory syncytial virus *in vitro*. However, the effectiveness of KD-1 in the treatment of CoV is not confirmed, and its mechanisms of action remain obscure. Accordingly, we evaluated the antiviral and anti-inflammatory efficiencies of KD-1 against a clinical isolate of SARS-CoV-2 and human coronavirus 229E (HCoV-229E) *in vitro* to explain the mechanisms of treatment of viral-induced inflammatory and develop the clinical use of KD-1.

In the present study, the antiviral and anti-inflammatory effects of KD-1 on SARS-CoV-2 and HCoV-229E infection *in vitro* were comprehensively evaluated. Results demonstrated that KD-1 inhibited virus replication in a dose-dependent manner. KD-1 could also markedly decrease the expression of proinflammatory cytokines in infected human hepatocellular carcinoma cell lines (Huh-7) by inhibiting the transcription factor nuclear factor kappa B (NF- $\kappa$ B) signal in Huh-7 cells. Our finding can help elucidate the mechanism of KD-1 against SARS-CoV-2 and HCoV-229E infection.

## Materials and methods

### Reagents

The KD-1 (lot: 20,190,201) used in this study was produced and provided by Dalian Fusheng Natural Medicine Development Co. Ltd. (Dalian, China). KD-1 was triturated, and 100 mg was prepared in 1 ml of dimethyl sulfoxide (DMSO). The mixture was ultrasonicated and then centrifuged. The supernatant was passed through a 0.22  $\mu$ m syringe filter before use.  $\kappa$ B $\alpha$  rabbit monoclonal (lot: 4812), p- $\kappa$ B $\alpha$  rabbit monoclonal (lot: 2859), NF- $\kappa$ B p65 rabbit monoclonal (lot: 8242), and p-NF- $\kappa$ B p65 rabbit monoclonal (lot: 3033) antibodies were provided by Cell Signaling Technology, Inc. (Danvers, MA, USA).

**Table 1**  
Primer sequence for RT-qPCR.

Target Gene	Direction	Sequence (5'–3')
IL-1 $\beta$	Forward	GCACGATGCACCTGTACGAT
	Reverse	AGACATCACCAAGCTTTTTTGTCT
	Probe	FAM-ACTGAACCTGCACGCTCCGGGACTC-TAM
TNF- $\alpha$	Forward	AACATCCAACCTTCCCAAAACG
	Reverse	GACCCCTAAGCCCCCAATTCTC
	Probe	FAM-CCCCCTCCTTCAGACACCCCTCAACC-TAM
IL-6	Forward	CGGGAACGAAGAGAAGCTCTA
	Reverse	CGCTTGTGGAGAAGGAGTTCA
	Probe	FAM-TCCCTCCAGGAGCCAGCT-TAM
MCP-1	Forward	CAAGCAGAAGTGGGTTTCAGGAT
	Reverse	AGTGAGTGTTCAGTCTTCGGAGTT
	Probe	FAM-CATGGACCACCTGGACAAGCAAACC-TAM
IP-10	Forward	GAAATTATTCTGCAAGCCAATTT
	Reverse	TCACCCCTCTTTTCAT-TGTAGCA
	Probe	FAM-TCCACGTTGTGAGATCA-TAM
GAPDH	Forward	GAAGGTGAAGGTCGGAGTC
	Reverse	GAAGATGGTGTGGGATTTTC
	Probe	CAAGCTTCCCGTTCTCAGCC-TAM

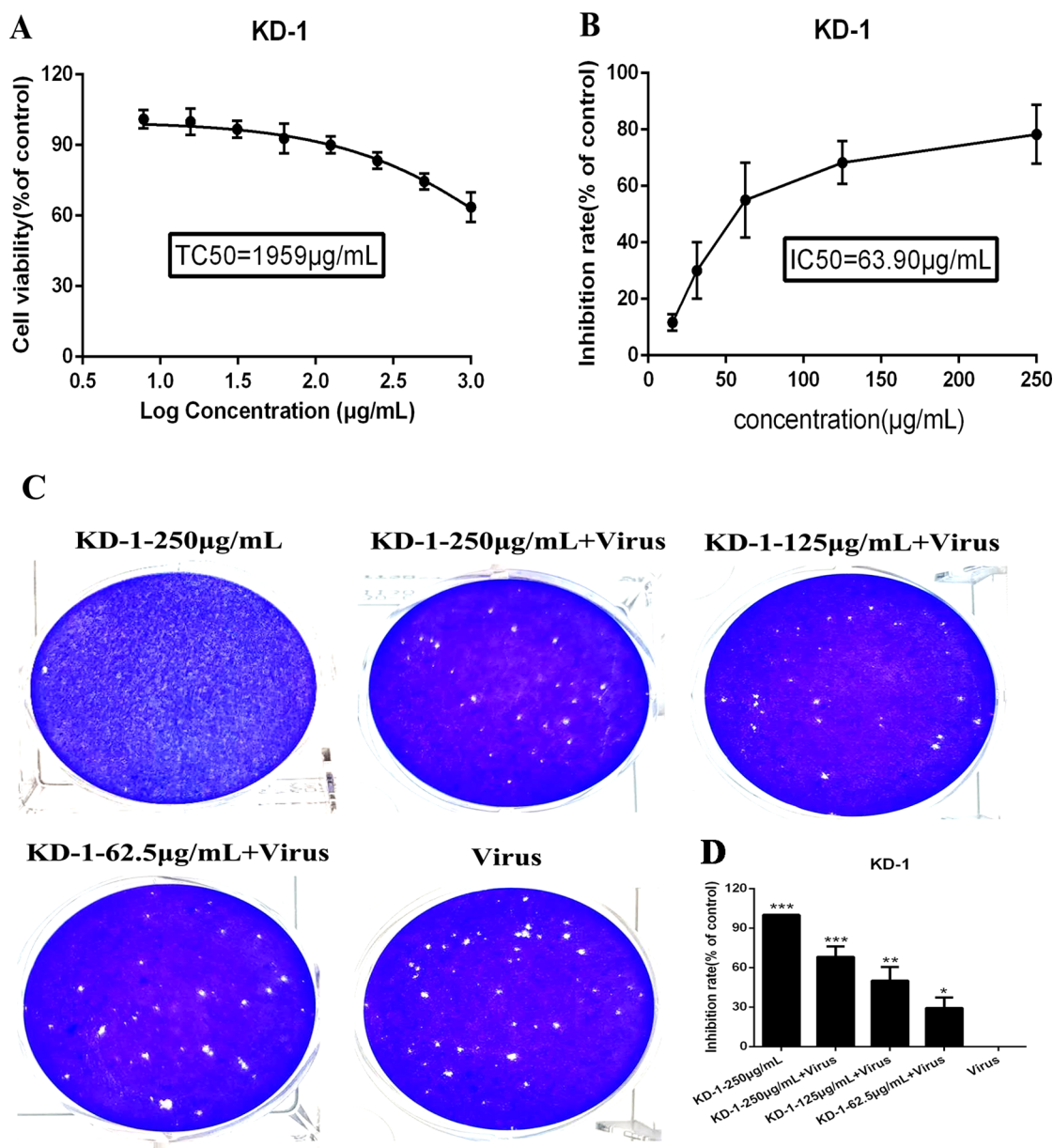


**Fig. 1.** Dose-dependent reduction of SARS-CoV-2-induced cytopathic effect and plaque formation by KD-1. Vero E6 cells were not-infected or infected with SARS-CoV-2 and the inhibitory effect of different concentrations of KD-1 on virus proliferation was evaluated. A. The cytotoxicity effects of KD-1 in Vero E6 cells was detected using MTT assay. (B) The inhibitory effects of KD-1 on SARS-CoV-2 in Vero E6 cells. (C) Inhibitory effect of KD-1 on plaque formation of SARS-CoV-2. (D) The quantitative analysis of the plaque formation in different groups was analyzed by SPSS ver. 19.0. Data were presented as the mean  $\pm$  SD obtained from three separate experiments. \*  $p < 0.05$ ; \*\*  $p < 0.01$ ; \*\*\*  $p < 0.001$ , compared with SARS-CoV-2-infected cells.

#### Cell lines and virus

African green monkey kidney epithelial (Vero E6) cells and human hepatocellular carcinoma cell lines (Huh-7) were purchased from ATCC. The cells were cultured in Dulbecco's modified Eagle's medium (DMEM, Gibco, USA) with 10% fetal bovine serum (FBS), 100 U/ml penicillin, and 100  $\mu\text{g/ml}$  streptomycin. The SARS-CoV-2 (Genbank accession no. MT123290.1) was clinically isolated from the First Affiliated Hospital of Guangzhou Medical University, and HCoV-229E (ATCC<sup>®</sup>VR740<sup>™</sup>) was purchased from ATCC. The viruses were propagated and adapted as previously described (Zhu et al., 2020). The 50% tissue culture infective dose (TCID<sub>50</sub>) of SARS-CoV-2 and HCoV-229E were determined using the Reed–Muench method (TCID<sub>50</sub> =  $10^{-6}$ /100  $\mu\text{l}$  and TCID<sub>50</sub> =  $10^{-5.5}$ / $\mu\text{l}$ , respectively). Virus stocks were collected and stored at  $-80^\circ\text{C}$ . The infection experiments of SARS-CoV-2 were performed in a biosafety level-3 laboratory and those of HCoV-

229E were performed in a biosafety level-2 laboratory.

#### Cytotoxicity assay

The cytotoxic effects of the KD-1 on Vero E6 and Huh-7 cells were evaluated by MTT assay (Park et al., 2011). Briefly, Vero E6 ( $5 \times 10^4$  cells/well) and Huh-7 ( $5 \times 10^4$  cells/well) cells grown in monolayer in 96-well plates were rinsed with PBS followed by incubation with indicated concentrations of KD-1. After 72 h, the cells were stained with 0.5 mg/ml MTT solution for 4 h. The supernatants were removed, and the formed formazan crystals were dissolved in 100  $\mu\text{l}$  of DMSO. The absorbance at 570 nm was determined using a Multiskan Spectrum reader (Thermo Fisher, USA). The 50% toxicity concentration (TC<sub>50</sub>) of KD-1 causing 50% death of cells was calculated.



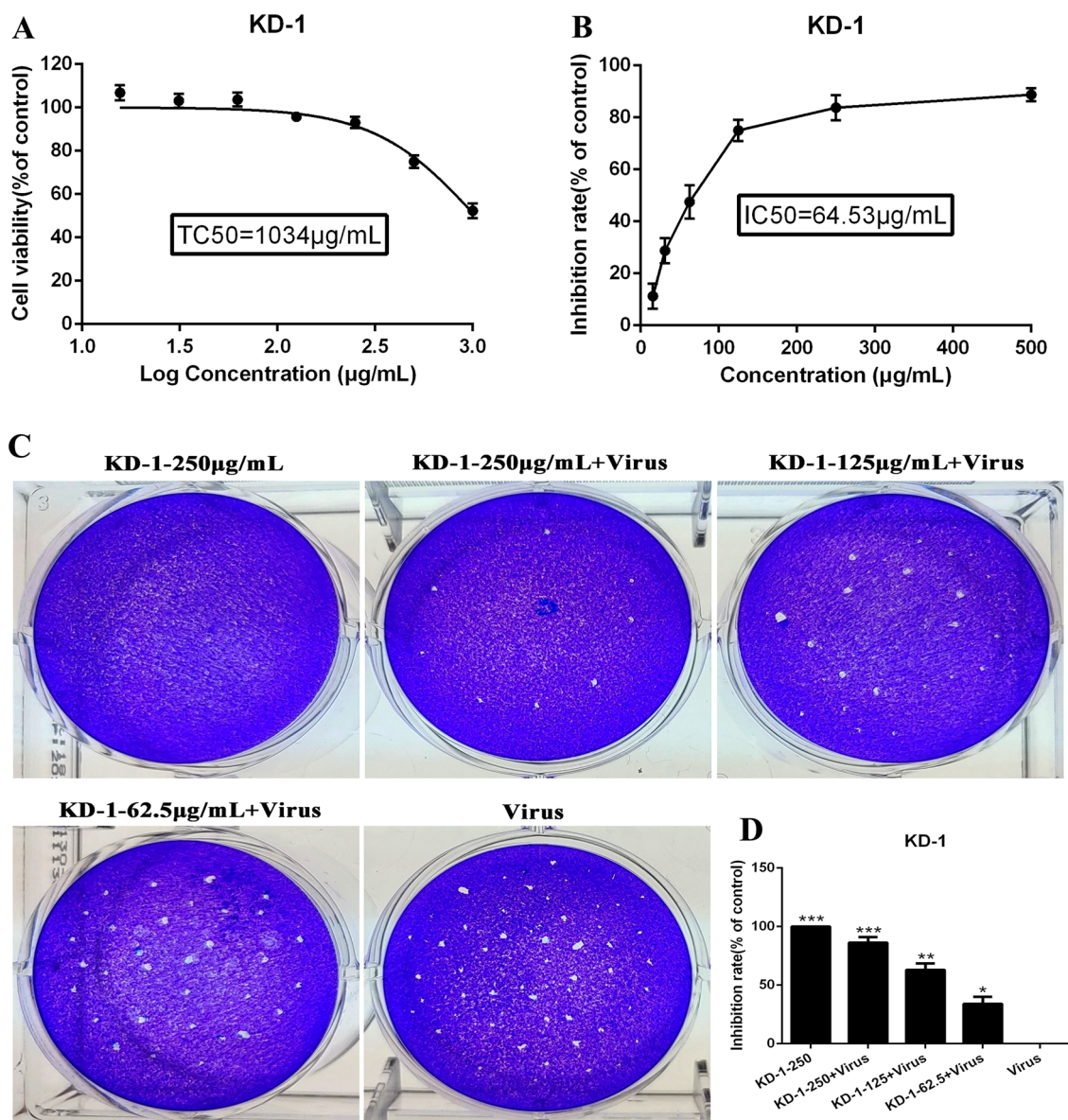


**Fig. 2.** Dose-dependent reduction of HCoV-229E-induced cytopathic effect and plaque formation by KD-1. Huh-7 cells were not-infected or infected with HCoV-229E and the inhibitory effect of different concentrations of KD-1 on virus proliferation was evaluated. A. The cytotoxicity effects of KD-1 in Huh-7 cells was detected using MTT assay. (B) The inhibitory effects of KD-1 on HCoV-229E in Huh-7 cells. (C) Inhibitory effect of KD-1 on plaque formation of HCoV-229E. (D) The quantitative analysis of the plaque formation in different groups was analyzed by SPSS ver. 19.0. Data were presented as the mean  $\pm$  SD obtained from three separate experiments. \*  $p < 0.05$ ; \*\*  $p < 0.01$ ; \*\*\*  $p < 0.001$ , compared with HCoV-229E -infected cells.

#### Cytopathic effect (CPE) inhibition assay

To investigate the antiviral effects of KD-1 against SARS-CoV-2 and HCoV-229E, we performed CPE inhibition assay with a nontoxic concentration of KD-1. Briefly, Vero E6 cell monolayers were grown in 96-well plates and inoculated with 100 TCID<sub>50</sub> of CoV strains at 37 °C for 2 h. The inoculum was removed, and the cells were subsequently incubated with indicated concentrations of KD-1. Following 72 h of incubation, the infected cells showed 100% CPE under a microscope. The percentage of CPE in KD-1-treated cells was recorded. The 50% inhibition concentration (IC<sub>50</sub>) of the virus-induced CPE by KD-1 was calculated as described, and the selectivity index (SI) was determined from the ratio of TC<sub>50</sub> to IC<sub>50</sub> (Reed et al., 1938).

#### Plaque-reduction assay

Plaque-reduction assay was performed as previously described.

Briefly, monolayer Vero E6 cells in 6-well plates were rinsed with PBS and incubated with 100 plaque-forming unit of SARS-CoV-2 and HCoV-229E. Following 2 h of incubation, the inoculum was removed and the cells were overlaid by 2 ml of agar/basic medium mixture, which contained 0.8% agar and indicated concentrations of KD-1. The plates were then incubated in 37 °C for 72 h, followed by fixation with 4% formalin for 30 min. The overlays were then removed and stained with 0.1% crystal violet for 3 min. The plaques were visualized and counted (Reed et al., 1938).

#### RNA isolation and reverse-transcriptase-quantitative PCR analysis (RT-qPCR)

To determine the possible mechanisms underlying the antiviral activity of KD-1, we used several drug concentrations with high antiviral efficiency for subsequent experiments. The primers of TNF- $\alpha$ , IL-6, MCP-1, IL-1 $\beta$ , IP-10, and GAPDH genes (Table 1) were designed using

## SARS-CoV-2

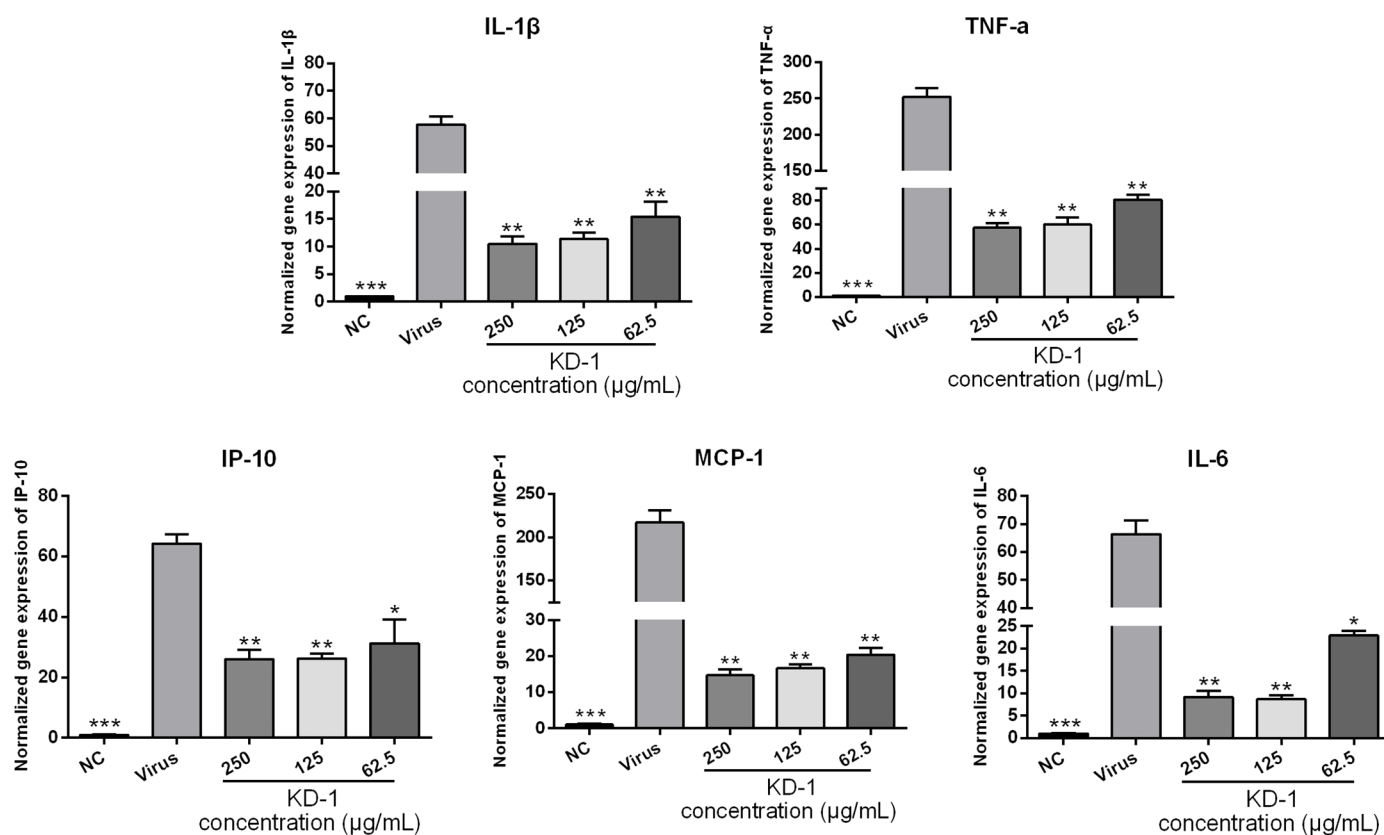


Fig. 3. Effects of KD-1 treatment on the mRNA expression levels of inflammatory mediators in SARS-CoV-2-infected Huh-7 cells. TNF- $\alpha$ , IL-1 $\beta$ , IL-6, IP-10, and MCP-1. Data were presented as the mean  $\pm$  SD obtained from three separate experiments. \*  $p < 0.05$ ; \*\*  $p < 0.01$ ; \*\*\*  $p < 0.001$ , compared with SARS-CoV-2-infected cells.

### Primer 5.0.

Briefly, Huh-7 cells grown in 12-well plates were rinsed with PBS and then exposed to CoV at a multiplicity of infection (MOI) of 1 for 2 h. The inoculums were removed after infection, and the cells were divided into the following six groups: normal control group (NC), virus-infected group (virus), and three groups with various of KD-1 concentrations. The cells were harvested at 48 h. Total RNA from the different groups was extracted in accordance with the specification of RNA reagent (Invitrogen, MA, USA), and reverse transcription of RNAs was quantified by using the PrimeScript™ RT Master Mix kit (Takara Bio, Japan). RT-PCR was then performed on cDNA samples by using SYBR Premix Ex Tap™ II (Takara Bio, Japan). PCR data were analyzed with ABI PRISM® 7500 Real-time PCR detection system (Applied Biosystems Co., USA). The relative amount of PCR products was calculated using the  $2^{-\Delta\Delta Ct}$  method as previously described (Pfaffl et al., 2001).

### Western blot assay

Huh-7 cells were treated as described in the “RNA isolation and reverse-transcriptase quantitative PCR analysis (RT-qPCR)” section and harvested for western blot analysis. Total proteins of the samples were extracted from the cells by lysis with radioimmunoprecipitation assay (RIPA) buffer (DGCS Biotechnology, China). The protein contents of the samples were determined by using the BCA kit (Beyotime, China). Then, 20 mg of the cell lysate was separated by 10% sodium dodecyl sulfate polyacrylamide gel electrophoresis (SDS-PAGE), and the separated proteins were transferred onto a polyvinylidene fluoride (PVDF) membrane (Millipore, USA). The membranes were blocked with 5% BSA for 2 h and then incubated with primary antibodies over night at 4

°C. Subsequently, the membranes were incubated with appropriate secondary antibodies for 1 h at 25 °C. The immune complexes were then immunoblotted with an HRP-conjugated anti-rabbit immunoglobulin-G antibody. Immunodetection was performed by using the enhanced chemiluminescence reagents (Fdbio, China). All experiments were repeated three times.

### Data analysis

All data in this study were analyzed by using analysis of variance (ANOVA) with SPSS ver. 19.0 (Armonk, NY, USA). Data were presented as the mean  $\pm$  standard deviation. Differences in multiple groups were determined by one-way ANOVA analysis of variance with Tukey's honest significant difference (HSD) test.  $P$ -value  $< 0.05$  was considered statistically significant.

## Result

### KD-1 exerted antiviral on SARS-CoV-2 and HCoV-229E in vitro

The cytotoxicity of KD-1 in Vero E6 and Huh-7 cells was evaluated by non-radioactive cell proliferation assay (MTT). The  $TC_{50}$  values corresponding to 50% cytotoxic effect after 72 h of inhibitor treatment were determined. The  $TC_{50}$  of KD-1 toward Vero E6 and Huh-7 cells were 1959  $\mu$ g/ml and 1034  $\mu$ g/ml, respectively (Figs. 1A and 2A). The antiviral activities of KD-1 against SARS-CoV-2 (Fig. 1) and HCoV-229E (Fig. 2) were evaluated by CPE inhibition assay. Results showed that KD-1 (250  $\mu$ g/ml, 125  $\mu$ g/ml and 62.5  $\mu$ g/ml) significantly reduced the CPE caused by infection in Vero E6 cells. Meanwhile, 31.25 and

## HCoV-229E

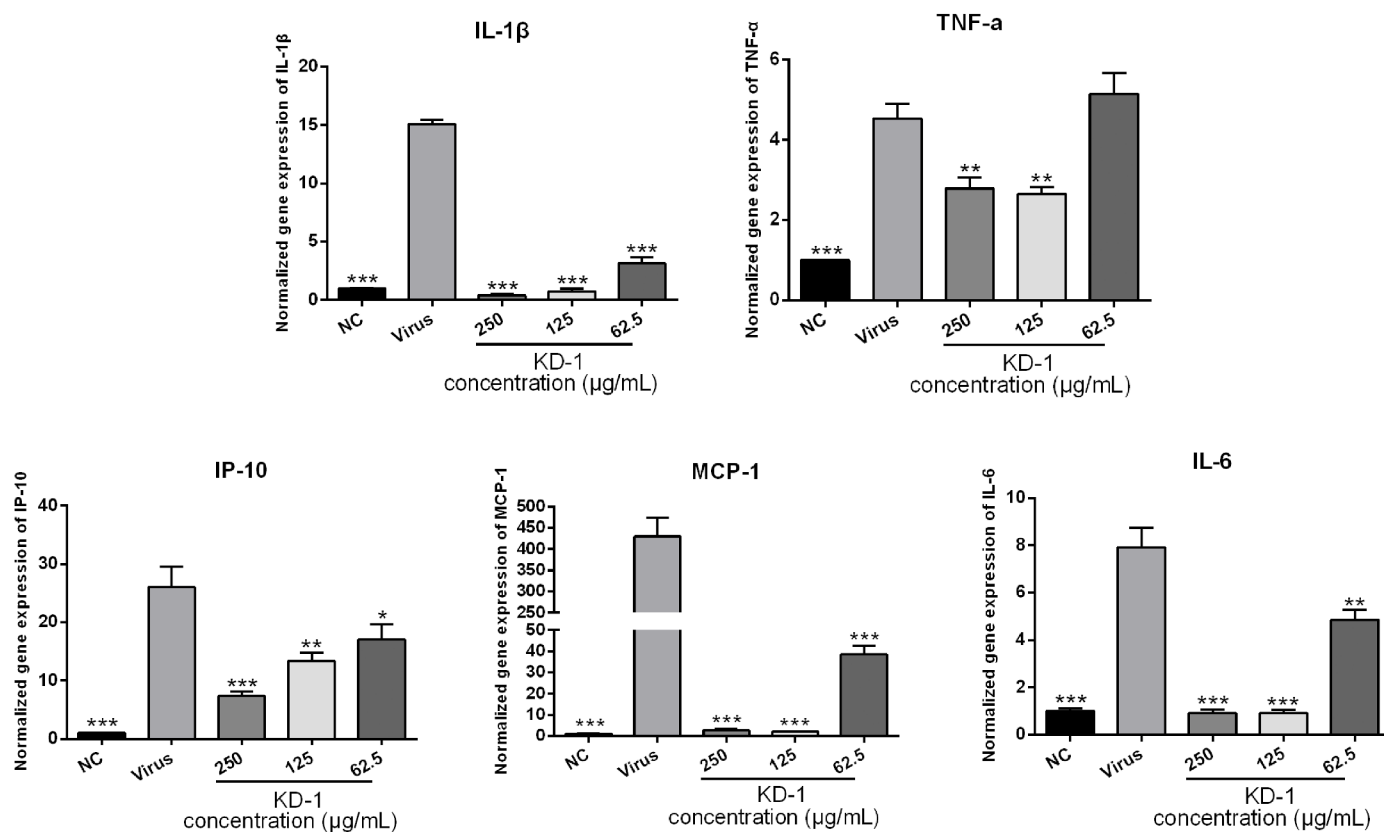


Fig. 4. Effects of KD-1 treatment on the mRNA expression levels of inflammatory mediators in HCoV-229E-infected Huh-7 cells. TNF- $\alpha$ , IL-1 $\beta$ , IL-6, IP-10, and MCP-1. Data were presented as the mean  $\pm$  SD obtained from three separate experiments. \*  $p < 0.05$ ; \*\*  $p < 0.01$ ; \*\*\*  $p < 0.001$ , compared with HCoV-229E-infected cells.

15.63  $\mu\text{g/ml}$  KD-1 were less active, and the  $\text{IC}_{50}$  value of KD-1 was 63.90  $\mu\text{g/ml}$ . The SI of KD-1 was 30.66 (Fig. 1B). The antiviral activity of KD-1 toward HCoV-229E was effective. The  $\text{IC}_{50}$  value of KD-1 toward HCoV-229E was 64.53  $\mu\text{g/ml}$  (Fig. 2B). The SI of KD-1 was 16.02. These results showed that KD-1 could protect cells from virus-induced cell death in a dose-dependent manner, and that the antiviral capability of KD-1 on SARS-CoV-2 was better than that on HCoV-229E.

A plaque-reduction assay was conducted to confirm the efficacy of KD-1 on SARS-CoV-2 (Fig. 1C and 1D) and HCoV-229E (Fig. 2C and 2D) propagation. Vero E6 and Huh-7 cells were infected with SARS-CoV-2 (MOI=0.1) and HCoV-229E (MOI=0.1), respectively. The cells were also incubated with overlay medium containing various KD-1 concentrations. After 3 days, the overlays were removed and stained with 0.1% crystal violet. The plaques were visualized and counted. Results showed that the average size and plaque number in KD-1-treated cells were markedly reduced in a dose-dependent manner. CPE and plaque-reduction assays showed that KD-1 may be a key parameter influencing SARS-CoV-2 and HCoV-229E activities.

#### KD-1 strongly inhibited the expression of proinflammatory cytokines in vitro

Infections by CoVs (including SARS-CoV-2 and HCoV-229E) can induce a strong inflammatory reaction, as hallmarked by the production of cytokines and chemokines. Accordingly, the influence of KD-1 on infected cells was examined by measuring cytokines. To determine the influence of KD-1 on the expression of proinflammatory cytokines induced by SARS-CoV-2 and HCoV-229E, the mRNA expression levels of IL-6, TNF- $\alpha$ , IL-1 $\beta$ , IP-10, and MCP-1 in Huh-7 cells were detected by RT-qPCR. As shown in Figs. 3 and 4, the mRNA expression levels of IL-

6, TNF- $\alpha$ , IL-1 $\beta$ , IP-10, and MCP-1 in the virus group were significantly up-regulated 48 h after infection in Huh-7 cells infected by SARS-CoV-2 ( $p < 0.01$ ) and HCoV-229E ( $p < 0.001$ ) compared with those in the NC group. Compared with the SARS-CoV-2 and HCoV-229E groups, KD-1 significantly reduced the mRNA expression levels of IL-6, TNF- $\alpha$ , IL-1 $\beta$ , IP-10, and MCP-1 in a dose-dependent manner in Huh-7 cells 48 h after infection ( $p < 0.01$  or  $p < 0.05$ ), respectively. This finding indicated that KD-1 may be an effective anti-inflammatory agent.

#### KD-1 significantly decreased the expression of key proteins related to the NF- $\kappa\text{B}$ signaling pathway in vitro

To further explore the mechanisms underlying the antiviral activity of KD-1, we examined the expression of proteins related to NF- $\kappa\text{B}$  signaling in Huh-7 cells infected by SARS-CoV-2 and HCoV-229E. Western blot analysis was performed using the cell lysates of Huh-7 cells treated with or without KD-1 to analyze the protein expression levels of NF- $\kappa\text{B}$  p65, p-NF- $\kappa\text{B}$  p65, I $\kappa\text{B}\alpha$ , and p-I $\kappa\text{B}\alpha$ . As shown in Figs. 5 and 6, the expression levels of NF- $\kappa\text{B}$  p65, p-NF- $\kappa\text{B}$  p65, and p-I $\kappa\text{B}\alpha$  of the virus group were markedly higher than those of the NC group ( $p < 0.01$ ), and the expression levels of I $\kappa\text{B}\alpha$  of the virus group were markedly lower than those of the NC group ( $p < 0.01$ ). Compared with the virus group, the protein expression levels of the NF- $\kappa\text{B}$  p65, p-NF- $\kappa\text{B}$  p65 were significantly reduced in Huh-7 cells with KD-1 (250, 125, and 62.5  $\mu\text{g/ml}$ ), and p-I $\kappa\text{B}\alpha$  was significantly reduced in Huh-7 cells with KD-1 (250 and 125  $\mu\text{g/ml}$ ). Meanwhile, I $\kappa\text{B}\alpha$  was significantly up-regulated in Huh-7 cells with KD-1 (250, 125, and 62.5  $\mu\text{g/ml}$ ).

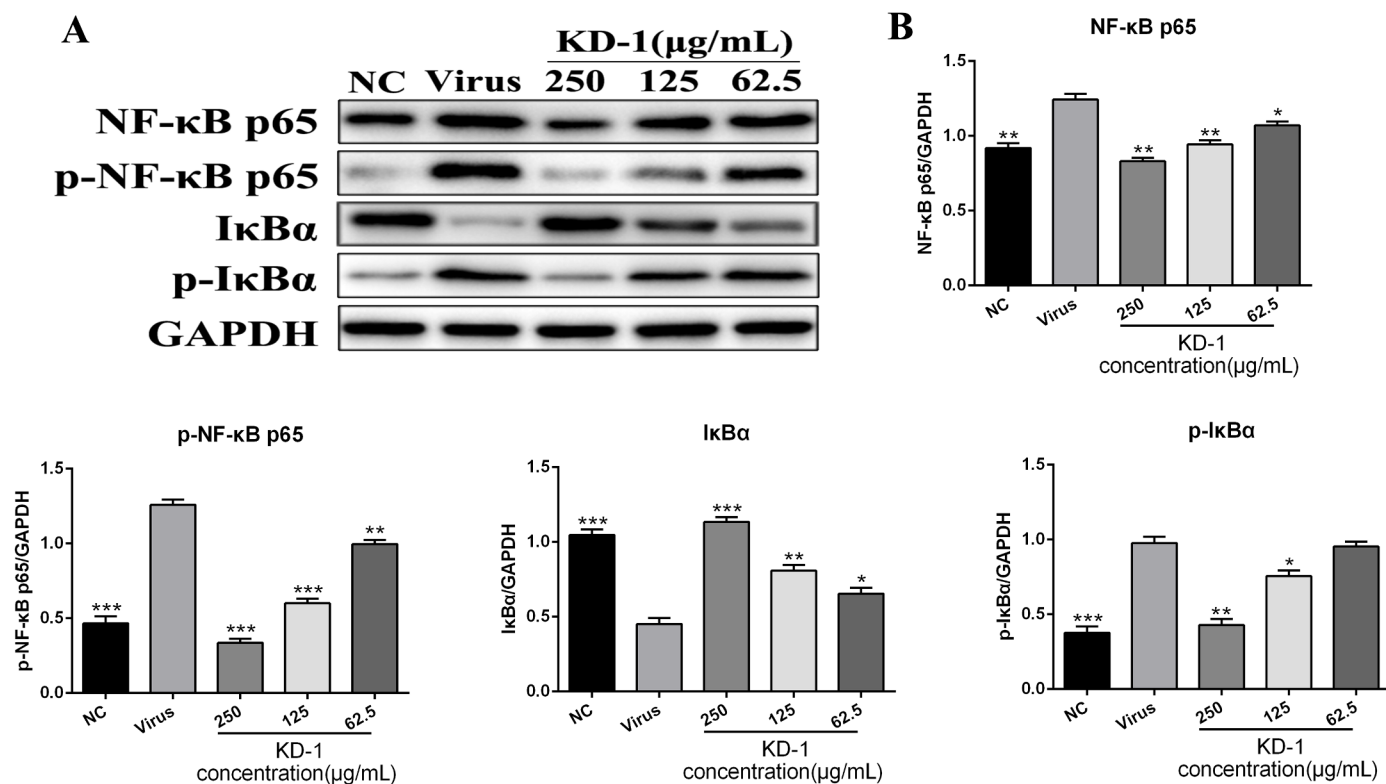


**Fig. 5.** KD-1 inhibits the inflammation induced by the virus through modulating the NF- $\kappa$ B pathway *in vitro*. (A) The expression of the NF- $\kappa$ B p65, p-NF- $\kappa$ B p65, p-I $\kappa$ B $\alpha$  and I $\kappa$ B $\alpha$  proteins in the Huh-7 cells was detected by western blot analysis; (B) The quantitative analysis of the NF- $\kappa$ B p65, p-NF- $\kappa$ B p65, p-I $\kappa$ B $\alpha$  and I $\kappa$ B $\alpha$  proteins was analyzed by Image J. The values were presented as the means  $\pm$  S.D. of three individual experiments. \*  $p < 0.05$ ; \*\*  $p < 0.01$ ; \*\*\*  $p < 0.001$ , when compared to the viral control.

## Discussion

The number of infections caused by the newly emerged SARS-CoV-2 continues to rise sharply in China (CDC, 2020; WHO, 2020). The extensive and rapid spread of this virus in the world has caused an outbreak of acute infectious pneumonia (Guang et al., 2020). It is a major CoV infection that has threatened human life after SARS and MERS (Mahase, 2020). No specific antiviral drugs or vaccines can be used for this sudden and lethal disease, and the supportive care and nonspecific treatment of the patient is the only option to ameliorate the symptoms (Clercq, 2020; Russell et al., 2020; Zumla et al., 2020). Thus, effective and safe antiviral agents are urgently needed. Nowadays, the use of TCM is a popular and acceptable therapy, and many TCM prescriptions have been proven to exert obvious therapeutic effect on viruses by inhibiting their replication directly and improving the immune functions of the host organism. Thus, these prescriptions may be effective antiviral drugs. KD-1, a representative ingredient of *F. suspensa*, possesses anti-inflammatory, anti-oxidant, and antiviral activities. However, the antiviral and anti-inflammation effects induced by SARS-CoV-2 and HCoV-229E and the potential mechanisms of KD-1 in treating viral pneumonia are unclear. Herein, we investigated the potential antiviral and anti-inflammatory activities of KD-1 on SARS-CoV-2 and HCoV-229E. We elucidated for the first time that KD-1 could inhibit SARS-CoV-2 and HCoV-229E infection and significantly suppress the inflammation caused by SARS-CoV-2 and HCoV-229E by down-regulating pro-inflammatory cytokines through the inhibition of the NF- $\kappa$ B signal pathway.

The effects of KD-1 against SARS-CoV-2 (Fig. 1) and HCoV-229E (Fig. 2) *in vitro* were measured by CPE and plaque assays. Results showed that KD-1 could protect cells from virus-induced cell death and inhibit the average size and plaque number in KD-1-treated cells in a dose-dependent manner. The SI index of KD-1 on SARS-CoV-2 and

HCoV-229E reached 30.66 and 16.02, respectively. All these results confirmed that KD-1 may be a key parameter influencing its viral activity.

Highly pathogenic CoVs, such as SARS-CoV and MERS-CoV reportedly cause fatal pneumonia, which is mainly associated with rapid virus replication, massive inflammatory cell infiltration, and elevated proinflammatory cytokine/chemokine responses. Although the pathophysiology of fatal pneumonia caused by highly pathogenic CoVs is not completely understood, recent studies suggest the crucial role of cytokine storm in causing fatal pneumonia (Channappanavar et al., 2017). Previous studies have shown increased amounts of proinflammatory cytokines (e.g., IL-1 $\beta$ , IL-6, IP-10, and MCP-1) in sera of SARS patients (Leong et al., 2006), which was similar in the serum of MERS patients with increased concentrations of proinflammatory cytokines (IFN- $\gamma$ , TNF- $\alpha$ , IL-15, and IL-17) (Assiri et al., 2013). Moreover, it was reported that the occurrence of cytokine storm in NCIP patients in the ICU but not in non-ICU patients (Huang et al., 2020). They detected the production of IL-1 $\beta$ , TNF- $\alpha$ , MCP-1, IP-10, and IL-6 induced by SARS-CoV-2 and HCoV-229E. Meanwhile, our results showed that KD-1 inhibited the release of IL-1 $\beta$ , TNF- $\alpha$ , MCP-1, IP-10, and IL-6 induced by SARS-CoV-2 and HCoV-229E in Huh-7 cells (Fig. 3 and Fig. 4) in a dose-dependent manner.

The SARS syndrome is characterized by uncontrolled inflammatory response, and NF- $\kappa$ B is the major transcription factor activated in acute respiratory distress syndrome (Fan et al., 2001). Similar to SARS-CoV, SARS-CoV-2 can also cause severe respiratory illness and even death. We performed RNA-seq of SARS-CoV-2 virus-infected Huh-7 cells using the Illumina HiSeq 2000 platform and found that SARS-CoV-2 infection could regulate the NF- $\kappa$ B, TNF and PI3K-Akt signaling pathway, as well as ECM-receptor interaction (data not shown). NF- $\kappa$ B plays an important role in mediating inflammation, immune responses, and other cellular activities (Mitchell et al., 2016). NF- $\kappa$ B activation can induce



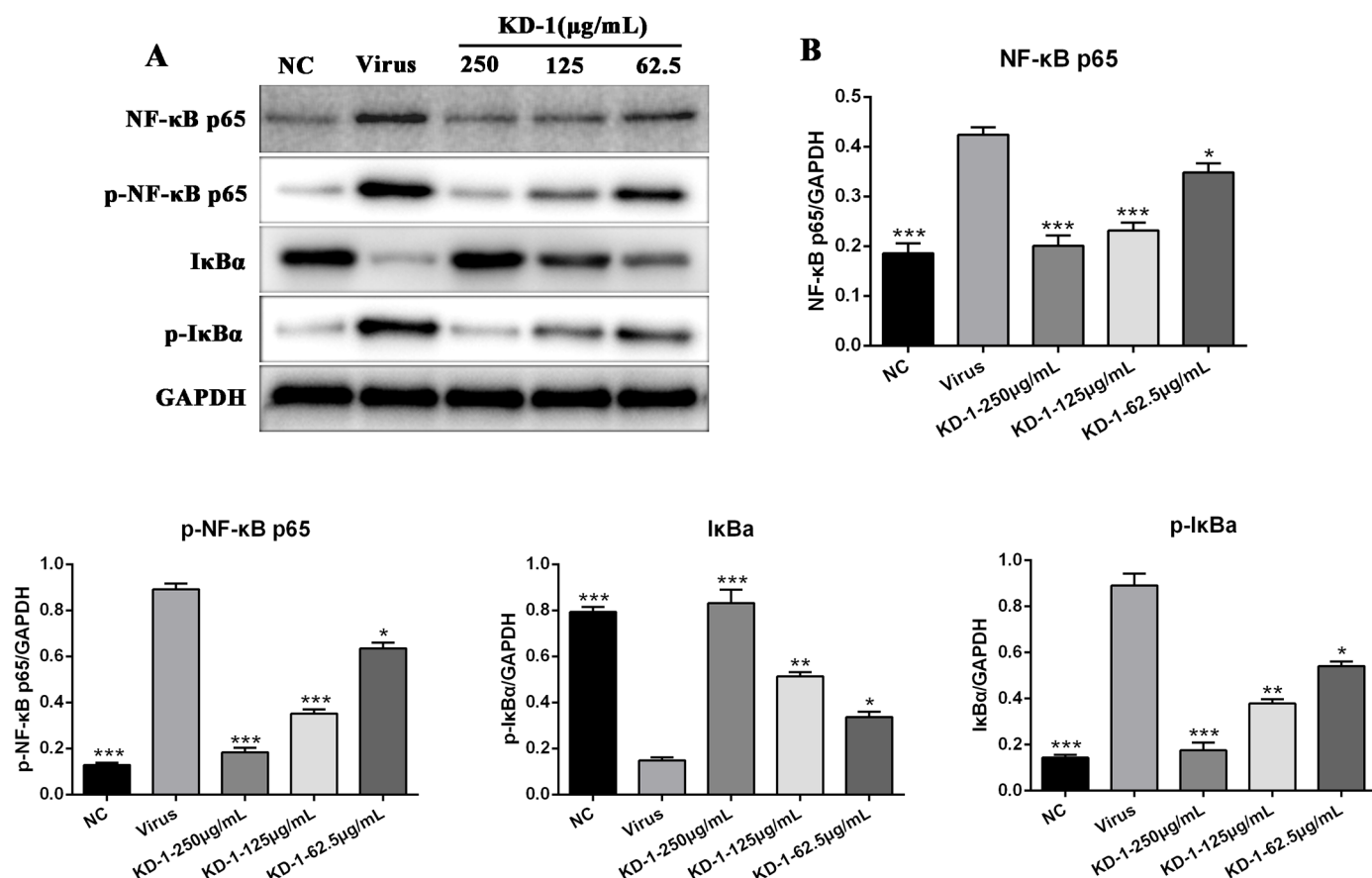


**Fig. 6.** KD-1 inhibits the inflammation induced by SARS-CoV-2 through modulating the NF-κB pathway *in vitro*. (A) The expression of the NF-κB p65, p-NF-κB p65, p-IκBα and IκBα proteins in the Huh-7 cells was detected by western blot analysis; (B) The quantitative analysis of the NF-κB p65, p-NF-κB p65, p-IκBα and IκBα proteins was analyzed by Image J. The values were presented as the means  $\pm$  S.D. of three individual experiments. \*  $p < 0.05$ ; \*\*  $p < 0.01$ ; \*\*\*  $p < 0.001$ , when compared to the viral control.

cytokine production, and these cytokines can react in turn, produce a positive autoregulatory loop and exacerbate the inflammatory response (Santoro et al., 2003). Accordingly, to understand the molecular mechanism of KD-1 action against CoV infection, we examined how the regulation of the NF-κB signaling pathway contributed to the alleviation of inflammation. Results showed that HCoV-229E activated the NF-κB signaling pathway, and that KD-1 could significantly decrease the HCoV-229E-induced activation of p-NF-κB p65 and p-IκBα, and increase the expression of IκBα (Figs. 5 and 6). We inferred that the mechanism underlying the antiviral activity of the KD-1 involved the impairment of the up-regulated pro-inflammatory cytokines induced by CoV by inhibiting the activity of the NF-κB signaling pathway. The change in cytokine profiles suggested that KD-1 may affect the inhibition of cytokine storm induced by CoV, and this deduction should be validated *in vivo*.

## Conclusions

Our results revealed that KD-1 could significantly protect cells from CoV-induced cell death and inhibit the average size and plaque number of the virus *in vitro*. The anti-CoV effect was attributed to the blocking of virus replication and the inhibition of the CoV-induced up-regulated expression of pro-inflammatory cytokines by a regulating the activity of the NF-κB signaling pathway. Thus, further evaluation of KD-1 as an anti-SARS-CoV-2 agent is needed. Our finding can serve as a reference to further reveal the mechanisms underlying the anti-inflammatory activity of KD-1 and its potential use to treat SARS-CoV-2-induced inflammation.

## Author contributions

Qin Hai Ma and Zifeng Yang designed the study. Qin Hai Ma and Runfeng Li wrote the paper. Li Fu, Runfeng Li, Weiqi Pan, and Wenbo Huang collected the samples. Bin Liu, Yuqi Xie, Zhoulang Wang, Chufang Li and Haiming Jiang performed the tests. Jicheng Huang, Yongxia Shi, Jun Dai, Kui Zheng, Xiaobo Li, Min Hui, Li Fu and Qin Hai Ma analyzed the data. Zifeng Yang and Li Fu thoroughly revised the manuscript. All authors read and approved the final manuscript.

## Declaration of Competing Interest

The authors declare no conflict of interest. All data were generated in-house, and no paper mill was used. All authors agree to be accountable for all aspects of work ensuring integrity and accuracy.

## Acknowledgments

This work was supported by China Postdoctoral Science Foundation (2020T130028ZX), Department of Education of Guangdong Provincial (2020KZDZX1159), Science research project of the Guangdong Province (Nos. 2020B111110001), Macao Science and Technology Development Fund (0172/2019/A3), National Key R&D Program of China (2020YFC0842400), Foshan Science and Technology Bureau (2020001000206), China Evergrande Group, Jack Ma Foundation (2020-CMKYGG-02), National Key Technology R&D Program (2018YFC1311900) and Guangdong Science and Technology Foundation (2019B030316028).

## References

- Assiri, A., Al-Tawfiq, J.A., Al-Rabeeh, A.A., Al-Rabiah, F.A., Al-Hajjar, S., Al-Barrak, A., Flemban, H., 2013. Epidemiological, demographic, and clinical characteristics of 47 cases of Middle East respiratory syndrome coronavirus disease from Saudi Arabia: a descriptive study. *Lancet Infect. Dis.* 13 (9), 752–761.
- Carlos, W.G., Dela Cruz, C.S., Cao, B., Pansnick, S., Jamil, S., 2020. Novel Wuhan (2019-nCoV) coronavirus. *Am. J. Respir. Crit. Care Med.* 201 (4), P7–P8.
- CDC, China. Distribution of 2019-nCoV infection. <http://2019ncov.chinacdc.cn/2019-nCoV/> (accessed Feb 17, 2020).
- Chen, X.F., Zhang, J.Y., Xue, C.X., Chen, X.G., Hu, Z.D., 2004. Simultaneous determination of some active ingredients in anti-viral preparations of traditional Chinese medicine by micellar electrokinetic chromatography. *Biomed. Chromatogr.* 18, 673–680.
- Clercq GLED, 2020. Therapeutic options for the 2019 novel coronavirus (SARS-CoV-2). *Nat. Rev. Drug Discov.*
- Channappanavar, R., Perlman, S., 2017. Pathogenic human coronavirus infections: causes and consequences of cytokine storm and immunopathology. *Semin. Immunopathol.* 39 (5), 529–539.
- Coon, T.A., Mckelvey, A.C., Weathington, N.M., Birru, R.L., Lear, T., Leikauf, G.D., Chen, B.B., 2014. Novel PDE4 inhibitors derived from Chinese medicine Forsythia. *PLoS ONE* 9, e115937.
- Coleman, C.M., Sisk, J.M., Mingo, R.M., Nelson, E.A., JM2, White, Frieman, M.B., 2016. Abelson kinase inhibitors are potent inhibitors of severe acute respiratory syndrome coronavirus and middle east respiratory syndrome coronavirus fusion. *J. Virol.* 90, 8924–8933.
- Díaz Lanza, A.M., Abad Martínez, M.J., Fernández Matellano, L., Recuero Carretero, C., 2001. Lignan and phenylpropanoid glycosides from *Phillyrea latifolia* and their *in vitro* anti-inflammatory activity. *Planta Med.* 67, 219–223.
- Du Toit, A., 2020. Outbreak of a novel coronavirus. *Nat. Rev. Microbiol.* 18 (3), 123.
- Fan, J., Ye, R.D., Malik, A.B., 2001. Transcriptional mechanisms of acute lung injury. *Am. J. Physiol. Lung. Cell. Mol. Physiol.* 281, 1037–1050.
- Guo, H., Liu, A.H., Ye, M., Yang, M., Guo, D.A., 2007. Characterization of phenolic compounds in the fruits of *Forsythia suspensa* by high-performance liquid chromatography coupled with electrospray ionization tandem mass spectrometry. *Rapid Commun. Mass Spectrom.* 21, 715–729.
- Gulcin, I., Elias, R., Gepdiremen, A., Boyer, L., 2006. Antioxidant activity of lignans from fringe tree (*Chionanthus virginicus* L.). *Eur. Food Res. Technol.* 223, 759–767.
- Guan, W.J., Ni, Z.Y., Hu, Y., Liang, W.H., Ou, C.Q., He, J.X., Liu, L., Shan, H., Lei, C.L., Hui, D.S.C., Du, B., 2020. Clinical characteristics of 2019 novel coronavirus infection in China. *medRxiv* 2006, 20020974 2002.
- Heimdal, I., Moe, N., Krokstad, S., Christensen, A., Skanke, L.H., Nordbø, S.A., Døllner, H., 2019. Human coronavirus in hospitalized children with respiratory tract infections: a 9-year population-based study from Norway. *J. Infect. Dis.* 219 (8), 1198–1206.
- Huang, C., Wang, Y., Li, X., Ren, L., Zhao, J., Hu, Y., Zhang, L., Fan, G., Xu, J., Gu, X., Cheng, Z., Yu, T., Xia, J., Wei, Y., Wu, W., Xie, X., Yin, W., Li, H., Liu, M., Xiao, Y., Gao, H., Guo, L., Xie, J., Wang, G., Jiang, R., Gao, Z., Jin, Q., Wang, J., Cao, B., 2020. Clinical features of patients infected with 2019 novel coronavirus in Wuhan, China. *Lancet* 395, 497–506.
- Ksiazek, T.G., Erdman, D., Goldsmith, C.S., Zaki, S.R., Peret, T., Emery, S., Tong, S., Urbani, C., Comer, J.A., Lim, W., Rollin, P.E., Dowell, S.F., Ling, A., Humphrey, C.D., Shieh, W., Guarner, J., Paddock, C.D., Rota, P., Fields, B., DeRisi, J., Yang, J., Cox, N., Hughes, J.M., LeDuc, J.W., Bellini, W.J., Anderson, L.J., 2003. A novel coronavirus associated with severe acute respiratory syndrome. *N. Engl. J. Med.* 348, 1953–1966.
- Kaitai, Y., Mingyu, L., Xin, L., Jihan, H., Hongbin, C., 2020. Retrospective clinical analysis of treating pneumonia caused by new coronavirus infection with Chinese medicine lianhua clearing disease. *Chin. J. Exp. Trad. Med. Formulae* 1–7.
- Lee, D.G., Lee, S.M., Bang, M.H., Park, H.J., Lee, T.H., Kim, Y.H., Kim, J.Y., Baek, N.I., 2011. Lignans from the flowers of *Osmanthus fragrans* var. *aurantiacus* and their inhibition effect on NO production. *Arch. Pharm. Res.* 34, 2029–2035.
- Leong, H.N., Chan, K.P., Oon, L.L., Koay, E., Ng, L.C., Lee, M.A., Barkham, T., Chen, M.I., Heng, B.H., Ling, A.E., 2006. Clinical and laboratory findings of SARS in Singapore. *Ann. Acad. Med. Singap.* 35 (5), 332–339.
- Lua, T., Piao, X.L., Zhang, Q., Wang, D., Piao, X.S., Kim, S.W., 2010. Protective effects of *Forsythia suspensa* extract against oxidative stress induced by diquat in rats. *Food Chem. Toxicol.* 48, 764–770.
- Mahase, E., 2020. China coronavirus: WHO declares international emergency as death toll exceeds 200. *BMJ* 368, m408.
- Mitchell, S., Vargas, J., Hoffmann, A., 2016. Signaling via the NF- $\kappa$ B system. *Wiley Interdiscip. Rev. Syst. Biol. Med.* 8, 227–241.
- Nkengasong, J., 2020. China's response to a novel coronavirus stands in stark contrast to the 2002 SARS outbreak response. *Nat. Med.* 26, 310–311.
- Owusu, M., Annan, A., Corman, V.M., Larbi, R., Anti, P., Drexler, J.F., Agbenyega, O., Adu-Sarkodie, Y., 2014. Human coronaviruses associated with upper respiratory tract infections in three rural areas of Ghana. *PLoS ONE* 9 (7), e99782.
- Pan, X., Cao, X., Li, N., Xu, Y., Wu, Q., Bai, J., Yin, Z., Luo, L., Lan, L., 2014. Forsythin inhibits lipopolysaccharide-induced inflammation by suppressing JAK-STAT and p38 MAPK signaling and ROS production. *Inflamm. Res.* 63, 597–608.
- Park, K.I., Park, H.S., Kang, S.R., Nagappan, A., Lee, D.H., Kim, J.A., Han, D.Y., Kim, G.S., 2011. Korean *Scutellaria baicalensis* water extract inhibits cell cycle G1/S transition by suppressing cyclin D1 expression and matrix-metalloproteinase-2 activity in human lung cancer cells. *J. Ethnopharmacol.* 133, 634–641.
- Pfaffl, M.W., 2001. A new mathematical model for relative quantification in real-time RT-PCR. *Nucleic. Acids. Res.* 29, e45.
- Reed, L.J., Muench, H., 1938. A simple method of estimating fifty percent endpoints. *Am. J. Epidemiol.* 27, 493–497.
- Russell, C.D., Millar, J.E., Baillie, J.K., 2020. Clinical evidence does not support corticosteroid treatment for SARS-CoV-2 lung injury. *Lancet North Am. Ed.*
- Santoro, M.G., Rossi, A., Amici, C., 2003. NF- $\kappa$ B and virus infection: who controls whom. *EMBO J.* 22, 2552–2560.
- WHO. Novel coronavirus (2019-nCoV) situation report-27 Feb 17, 2020. [https://www.who.int/docs/default-source/coronaviruse/situation-reports/20200216-sitrep-27-covid-19.pdf?sfvrsn=78c0eb78\\_2](https://www.who.int/docs/default-source/coronaviruse/situation-reports/20200216-sitrep-27-covid-19.pdf?sfvrsn=78c0eb78_2) (accessed Feb 17, 2020).
- Xu, X., Yu, C., Zhang, L., Luo, L., Liu, X., 2020. Imaging features of 2019 novel coronavirus pneumonia. *Eur. J. Nucl. Med. Mol. Imaging* 47, 1022–1023.
- Xia, S., Yan, L., Xu, W., Agrawal, A.S., Algaissi, A., Tseng, C.K., Wang, Q., Du, L., Tan, W., Wilson, I.A., Jiang, S., Yang, B., Lu, L., 2019. A pan-coronavirus fusion inhibitor targeting the HR1 domain of human coronavirus spike. *Sci. Adv.* 5 eaav4580.
- Zaki, A.M., van Boheemen, S., Bestebroer, T.M., Osterhaus, A.D., Fouchier, R.A., 2012. Isolation of a novel coronavirus from a man with pneumonia in Saudi Arabia. *N. Engl. J. Med.* 3671814–3671820.
- Zhong, W.T., Wu, Y.C., Xie, X.X., Zhou, X., Wei, M.M., Soromou, L.W., Ci, X.X., Wang, D.C., 2013. Phyllyrin attenuates LPS-induced pulmonary inflammation via suppression of MAPK and NF- $\kappa$ B activation in acute lung injury mice. *Fitoterapia* 90, 132–139.
- Zhu, N., Zhang, D., Wang, W., Li, X., Yang, B., Song, J., Zhao, X., Huang, B., Shi, W., Lu, R., Niu, P., Zhan, F., Ma, X., Wang, D., Xu, W., Wu, G., Gao, G.F., Tan, W., 2020. A novel coronavirus from patients with pneumonia in China, 2019. *N. Engl. J. Med.* 382 (8), 727–733.
- Zumla, A., Hui, D.S., Azhar, E.I., Memish, Z.A., Maeurer, M., 2020. Reducing mortality from host-directed therapies should be an option. *Lancet North Am. Ed.* 22 (395) 10224.